Journal of Cell Science 103, 965-976 (1992)
Printed in Great Britain © The Company of Biologists Limited 1992



# Brain microtubule-associated proteins modulate microtubule dynamic instability in vitro

## Real-time observations using video microscopy

NANCY K. PRYER*, RICHARD A. WALKER†, VICTORIA PETRIE SKEEN, BRENDA D. BOURNS‡, MICHAEL F. SOBOEIRO and EDWARD D. SALMON§

*Department of Biology, CB # 3280, Fordham Hall, University of North Carolina, Chapel Hill, NC 27599, USA*

*Present address: Division of Biochemistry and Molecular Biology, University of California, Berkeley, CA 94720, USA
†Present address: Department of Cell Biology, Duke University Medical Center, Durham, NC 27710, USA
‡Present address: Department of Pathology, University of Washington, Seattle, WA 98195, USA
§Author for reprint requests

### Summary

**We used video assays to study the dynamic instability behavior of individual microtubules assembled in vitro with purified tau, purified MAP2 or a preparation of unfractionated heat-stable MAPs. Axoneme-nucleated microtubules were assembled from pure tubulin at concentrations between 4 and 9 μM in the presence of MAPs, and observed by video-differential interference contrast microscopy. Microtubules co-assembled with each MAP preparation exhibited the elongation and rapid shortening phases and the abrupt transitions (catastrophe and rescue) characteristic of dynamic instability. Each MAP preparation increased the microtubule elongation rate above that for purified tubulin alone by decreasing the tubulin subunit dissociation rate during elongation. The brain MAPs used in this study reduced the rate of microtubule rapid shortening, but allowed significant loss of polymer during the shortening phase. Purified tau and MAP2 decreased the frequency of catastrophe and increased the frequency of rescue, while the heat-stable MAPs suppressed catastrophe at all but the lowest tubulin concentrations. Thus, each of these MAPs modulates, but does not abolish, dynamic instability behavior of microtubules. We propose a model to explain how MAP2 and tau bind to the microtubule lattice at sites along protofilaments so that the MAPs promote polymerization, but do not significantly block the mechanism of rapid shortening inherent in the tubulin lattice. Rapid shortening, when it occurs, proceeds primarily by the dissociation of short fragments of protofilaments, which contain the bound MAPs.**

Key words: microtubules, microtubule-associated proteins, dynamic instability, video microscopy.

### Introduction

Microtubule-associated proteins (MAPs) are a diverse collection of proteins that bind to microtubules. The collection of MAPs includes proteins that act as molecular motors (Vallee and Shpetner, 1990) and proteins that stimulate microtubule assembly (Vallee and Bloom, 1984; Olmsted, 1986), but the functional properties of most MAPs remain unknown. The abundant mammalian brain MAPs designated MAP1 (three proteins of about 350 kDa), MAP2 (199 kDa) and tau (55-62 kDa) were identified as the most prominent proteins that co-purify with tubulin through cycles of microtubule assembly and disassembly (Sloboda et al., 1976; Cleveland et al., 1977; Murphy et al., 1977; Vallee and Davis, 1983). The effects of these MAPs on microtubule assembly were originally studied by measuring the light-scattering generated by microtubule assembly in solution. In these studies, unfractionated brain MAPs stimulated the nucleation of microtubule assembly, increased the rate of microtubule elongation (Sloboda et al., 1976; Murphy et al., 1977), and decreased the rate of microtubule disassembly upon dilution (Job et al., 1985). These studies established the general effects of brain MAPs on populations of microtubules. However, the effects of individual, purified MAPs on microtubule assembly have not been well studied, particularly at the level of individual microtubule dynamic instability (Mitchison and Kirschner, 1984a).

Dynamic instability is the basic mechanism of microtubule assembly for purified tubulin in vitro (Mitchison and Kirschner, 1984a,b; Horio and Hotani, 1986; Walker et al., 1988; Simon and Salmon, 1992) and for the majority of microtubules of the interphase cytoplasmic microtubule complex and the mitotic spindle of dividing cells (Saxton

et al., 1984; Soltys and Borisy, 1985; Schulze and Kirschner, 1986; Cassimeris et al., 1987; Cassimeris et al., 1988; Sammak and Borisy, 1988; Schulze and Kirschner, 1988). Microtubules undergoing dynamic instability exist in two interconverting phases: the majority of microtubules are in a phase of relatively slow, steady elongation, while a smaller fraction of microtubules is in a phase of rapid shortening. Conversions between these phases are abrupt and stochastic, infrequent in comparison to the rates of subunit association and dissociation at microtubule ends, and depend on the free tubulin subunit concentration. On the basis of real-time video microscopic observations of individual microtubules assembled from purified tubulin, Walker et al. (1988) used the following terms to describe the phases and transitions of dynamic instability. The phases are termed *elongation* (net addition of subunits) and *rapid shortening* (net loss of subunits). The transitions between these phases are *catastrophe* - the transition from elongation to rapid shortening, and *rescue* - the transition from rapid shortening to elongation before complete disassembly has occurred. A third transition is *nucleation* - the initiation of microtubule assembly, which was observed using axonemes as nucleation centers. An accurate characterization of microtubule assembly requires determination of the rates of elongation and shortening and frequencies of transitions for microtubule dynamic instability.

The parameters of dynamic instability determined for microtubules assembled from purified tubulin probably do not represent microtubule dynamics in the cell, where microtubules interact with a number of different MAPs. Neuronal microtubules, which are the source for brain MAP preparations, appear to be much more stable than microtubules of mitotically active cells (Bamburg et al., 1986; Okabe and Hirokawa, 1988; Seitz-Tutter et al., 1988). This stability is not a property of brain tubulin itself, as microtubules assembled from purified brain tubulin are highly dynamic in vitro (Mitchison and Kirschner, 1984a). In contrast, microtubules assembled from purified brain tubulin in the presence of unfractionated brain MAPs exhibit little or no dynamic instability (Horio and Hotani, 1986; Farrell et al., 1987; Hotani and Horio, 1988). Length distributions of microtubules assembled in the presence of MAP2 or tau suggest that these microtubules undergo few rapid shortening events (Bre and Karsenti, 1990). However, the bulk solution assays of microtubule dynamics used in these studies cannot reveal MAP effects on the precise parameters of dynamic instability.

To understand how specific MAPs influence microtubule assembly, it is essential to investigate the effects of individual MAPs on the dynamic instability behavior of individual microtubule ends. We have used video contrast-enhanced differential interference contrast (DIC) microscopy and digital image processing (Salmon et al., 1989) to observe the assembly dynamics of individual ends of microtubules assembled from purified tubulin in the presence of brain MAPs. We began by using an unfractionated preparation of heat-stable brain MAPs (hs MAPs). This preparation, produced by boiling three-cycled microtubule protein, contains primarily MAP2 and tau, but a number of minor proteins are also present. To study the effects of individual MAPs, MAP2 and tau were purified by further fractionation of the hs MAP preparation. Our results show that the hs MAPs promote assembly and suppress catastrophe, resulting in stable microtubules, as shown previously for other preparations of unfractionated MAPs (Sloboda et al., 1976; Murphy et al., 1977; Job et al., 1985). Purified MAP2 and purified tau, added to tubulin in amounts previously determined to saturate microtubule binding sites (Cleveland et al., 1977; Kim et al., 1979), also promoted microtubule assembly. These MAPs enhanced nucleation, increased elongation velocity, suppressed catastrophe, and promoted rescue. At the tubulin concentrations used in this study (4-9 μM), frequent catastrophes and extensive rapid shortening occurred in the presence of MAP2 or tau, but not the hs MAPs. From these observations, we propose a model to explain how MAPs could bind to the microtubule lattice, promote microtubule assembly, and still permit dynamic instability behavior.

## Materials and methods

### *Purification of tubulin*

Porcine brain tubulin was purified to homogeneity by cycles of assembly and disassembly, followed by phosphocellulose chromatography and an additional cycle of assembly in the presence of 1 M $Na^+$ glutamate, as described previously (Walker et al., 1988). Purified tubulin was suspended in PM buffer (100 mM Pipes, pH 6.9, 2 mM EGTA, 1 mM $MgSO_4$, 1 mM GTP), frozen in liquid nitrogen, and stored at −80°C. The protein concentration, purity and fraction of active tubulin were determined as described (Walker et al., 1988).

We used two different preparations of purified tubulin in this study. Tubulin concentrations used in the video assays were adjusted to reflect the proportion of active tubulin in each preparation. Both tubulin preparations exhibited the same rate of elongation at a given active tubulin concentration. Tubulin preparation 1 was used in the hs MAP and tau studies, while MAP2 effects were studied with tubulin preparation 2. Both tubulin preparations used in the present study were also used to generate kinetic data on the dynamic instability of MAP-free microtubules in our previous paper (Walker et al., 1988). These data are presented again in Figs 2, 3, 4 and 5, and Table 1 of this paper.

### *Purification of MAPs*

Three different preparations of MAPs were purified from twice-cycled porcine brain microtubule protein (Sloboda et al., 1976). Heat-stable MAPs were prepared by the method of Kim et al. (1979), concentrated by ammonium sulfate precipitation, resuspended in PM buffer and dialyzed against PM buffer containing 0.1 mM PMSF. Tau was purified by two steps of ion-exchange chromatography. First, brain MAPs were separated from tubulin on a phosphocellulose column (Voter and Erickson, 1982) and stored at −80°C until further purification. These MAPs were later thawed, desalted over Sephadex G-25M (Pharmacia, Piscataway, NJ) and concentrated using a Centricon-30 filtration device (Amicon, Danvers, MA). MAPs were then loaded on a 12 ml, 1 cm diameter column of DEAE-Sephacel (Pharmacia) and eluted with PM buffer containing 0.1 mM PMSF. Under these conditions, tau appears in the flow-through fraction (Murphy et al., 1977). Tau-containing fractions were concentrated in a Centricon-30 device. MAP2 was isolated by boiling (Kim et al., 1979), followed by further purification on a 0.5 cm × 37 cm Bio-Gel A-15m (Bio-Rad Laboratories, Richmond, CA) gel filtration column (Voter and Erickson, 1982). All MAPs were stored frozen at −80°C until use.

A light-scattering assay was used to test MAP preparations for

the ability to stimulate microtubule assembly. MAPs (0.25 mg/ml) were combined with 20 μM (active concentration) purified tubulin. Microtubules did not self-assemble from MAP-free tubulin at this concentration. Light-scattering was monitored at 350 nm in a LKB Ultrospec 4050 spectrophotometer as the preparation was warmed to 37ºC. Each of the MAP preparations stimulated assembly of microtubules sufficient to generate 0.10 to 0.15 unit of absorbance at 350 nm (data not shown).

### *Saturation of MAP-binding sites on microtubules*

MAPs were added to tubulin in amounts more than sufficient to saturate microtubule MAP-binding sites. MAP:tubulin ratios were calculated as follows. First, for purified MAPs, we used published values for MAP saturation of microtubules to determine MAP:tubulin ratios. MAP2 has been estimated to bind to tubulin at a molar ratio of one MAP2 molecule per nine tubulin dimers (Kim et al., 1979). We used MAP2 at a molar ratio of one MAP2 per eight tubulin dimers, assuming a molecular mass of 290 kDa. However, the nucleotide sequence of MAP2 (Lewis et al., 1988) predicts a protein of 199 kDa, so that the ratio we used was closer to 1 MAP2 per 6 tubulin dimers. We confirmed that this ratio was sufficient for saturation by determining the amount of MAP2 bound to microtubules at several different MAP concentrations (methods adapted from Kim et al. (1979) and Hirokawa et al. (1988); data not shown). For tau, estimates of microtubule binding ratios range from one tau per ten tubulin dimers Cleveland et al. (1977) to one tau per five tubulin dimers Hirokawa et al. (1988). In our studies, tau was combined with tubulin at an approximate molar ratio of one tau per two tubulin dimers, assuming a molecular mass of 55 kDa for tau. The hs MAP fraction was added at a concentration 75% that of tubulin (on a w/w basis). For example, for 5 μM tubulin (0.5 mg/ml), hs MAPs were added to a final concentration of 0.375 mg/ml. MAP concentrations were scaled relative to tubulin concentration for each data point.

The amount of MAPs in our video assays is likely to be considerably above that needed for saturation, since the above MAP:tubulin molar ratios were calculated assuming that all the soluble tubulin assembled into polymer. However, in our video assays, assembly was limited by the small number of nucleation sites (axonemes), and a very small portion of the total tubulin was incorporated into microtubules. We estimate that about one per cent of the total tubulin was assembled into polymer. Thus, MAPs were present in great excess in comparison to the amount of tubulin assembled into microtubules.

Finally, MAPs in excess of the amounts determined above were added to compensate for non-specific MAP adhesion to the glass slide and coverslip. As described below, we determined that as much as 50% of the total MAP could be bound non-specifically to the coverslip at the MAP concentrations we used. To retain the appropriate MAP:tubulin ratios, we calculated how much MAP was expected to bind to the coverslip at each MAP concentration, and then added that amount to the final preparation. Thus, the final amount of free MAP was still in great excess of the estimated molar ratios required for saturation of microtubule MAP-binding sites (Kim et al. 1979; Cleveland et al., 1977; Hirokawa et al., 1988). After correcting for adsorption to glass surfaces, final free MAP2 concentrations were 0.75-1.2 μM, and tau concentrations ranged from 3 to 4.5 μM.

### *Experimental procedure*

#### *Standard video assays*

Purified fragments of sea urchin flagellar axonemes (Bell et al., 1982; Walker et al., 1988) provided the nucleation sites for microtubule assembly. Axonemes (final concentration of $2.7 \times 10^7$ axonemes/ml) were mixed with purified tubulin, MAPs and PM buffer and held on ice until use (not more than one hour).

Five μl of the MAP-tubulin-axoneme mixture was placed between a slide and biologically cleaned (Lutz and Inoue, 1986) coverslip (22 $mm^2$, thickness #0) and sealed with valap (vaseline:lanolin:paraffin, 1:1:1, by wt). Microtubule assembly in the slide-coverslip preparation was initiated by heating the microscope stage to 37 °C with a Sage model 279 air curtain incubator (Orion Research Inc., Cambridge, MA).

#### *Perfusion chamber video assay*

Dilution experiments were carried out using a low-volume flow cell designed for rapid exchange of solutions through the flow cell chamber (Berg and Block, 1984). The flow cell was assembled and used essentially as described previously (Walker et al., 1991). The microtubule assembly mixture was prepared by mixing tubulin and axonemes (at $2.7 \times 10^7$ axonemes/ml) with PM buffer, bringing the final tubulin concentration to 8 μM. When MAP2 was added to the assembly mixture, MAP2:tubulin ratios were the same as used in the standard video assays described above. The axoneme fragments provided the only nucleation sites for microtubule assembly, again limiting the amount of polymer assembled to 1% of the total tubulin subunit concentration. Self-assembly of microtubules was not observed under these conditions. The microtubule assembly mixture was placed into a partially assembled flow cell containing only the bottom coverslip, and sealed by the addition of the upper coverslip. The assembled flow cell was then placed on the microscope stage warmed to 37ºC, where the elevated temperature initiated microtubule assembly in the flow cell.

After 10 minutes of initial microtubule assembly, dilution of the tubulin subunit concentration was achieved by perfusing the flow cell for six seconds at a flow rate of 0.014 ml/s. Dilution solutions, warmed to 37ºC prior to perfusion, consisted of either PM buffer alone or PM buffer containing MAP2 at the same saturating concentrations used for assembly. We perfused the flow cell with dilution solution for a total of six seconds to ensure complete buffer exchange throughout the 50 μl volume of the chamber. Careful calibration of solution exchange at the surface of the coverslip established that six seconds of perfusion should be sufficient to dilute the free tubulin subunit concentration to about 15% of the initial concentration (Walker et al., 1991).

### *MAP adsorption to slide and coverslip surfaces*

We previously established that tubulin does not significantly adhere to the glass surfaces of our slide-coverslip preparation (Walker et al., 1988). However, MAP adsorption to the glass surfaces could decrease the amount of active MAPs available to interact with microtubules. We used fluorescence recovery after photobleaching (FRAP) to study MAP adsorption to coverslips. Heat-stable MAPs were labeled with 6-iodoacetamido fluorescein according to the procedure of Scherson et al. (1984). Labeled MAPs were diluted in PM to 0.25, 0.50, 0.75, 1.0 and 1.25 mg/ml and placed in our usual slide-coverslip preparation. The percentage of labeled MAPs remaining in solution was determined by FRAP analysis of the fluorescent label (in solution and on both glass surfaces) at 10, 20 and 30 minutes after construction of the slide-coverslip preparation. The FRAP methods used were those described by Wadsworth and Salmon (1986).

We found that MAPs adhere rapidly to glass surfaces, and that this binding saturates quickly. From the first time point at 10 minutes after slide-coverslip construction to 40 minutes after slide-coverslip construction, the amount of mobile fluorescently labeled MAPs did not change. However, the amount of labeled MAPs in solution increased with increasing MAP concentration. At 0.25 mg/ml MAP, only 25% of the fluorescent label was mobile. As the MAP concentration was raised to 0.5 mg/ml, 60% of the label was mobile. Above 0.75 mg/ml, 75-80% of the fluorescently labeled MAPs were mobile.

*Video microscopy and data analysis*

The microscopic methods used to visualize individual microtubules have been described previously (Pryer et al., 1986; Walker et al., 1988; Salmon et al., 1989).

Rates of elongation and rapid shortening and the duration of phases were measured as described (Walker et al., 1988). Changes in microtubule length were plotted as a function of time, and average rates of elongation and rapid shortening were determined by least squares regression analysis. Mean rates of elongation and rapid shortening for individual microtubules were determined by least squares regression analysis and then pooled for microtubules of each polarity, at each tubulin concentration, and averaged. Each data point in Figs 3, 4 and 5, and Table 1, represents a minimum of nine microtubules observed for a minimum of 10 minutes each. The average number of microtubules per point was 22, with a range of 9 to 59 individual microtubules tracked per point. An individual microtubule was designated plus or minus, based on the rate of elongation. We previously verified that the fast-growing microtubule end corresponds to the structural plus end in our assay system (Walker et al., 1988).

Frequencies of transition were calculated as described previously (Walker et al., 1988). For example, catastrophe frequency ($k_c$) was determined by summing the total time spent in elongation for all microtubules of one polarity at a single tubulin concentration and summing the total number of catastrophes that occurred during that time. Division of the total number of catastrophes by the total time in elongation yields $k_c$, expressed as catastrophes per second. The frequency of rescue ($k_r$) was calculated in the same way, using the time spent in rapid shortening and total number of rescues in that time.

## Results

*MAP-containing microtubules exhibit dynamic instability at both ends*

The observations reported in this paper used video assay methods that we developed previously (Pryer et al., 1986; Walker et al., 1988; Salmon et al., 1989) to visualize individual microtubules and characterize the parameters of spontaneous dynamic instability for microtubules assembled from purified tubulin in the presence of MAPs. Microtubules were assembled from purified tubulin in the presence of each of three different MAP preparations: purified MAP2 (0.75-1.2 μM), purified tau (3-4.5 μM), and hs MAPs (0.3-0.52 mg/ml), which are a mixture of MAP2, tau and other brain proteins resistant to heat denaturation. Over a range of tubulin concentrations, the MAP:tubulin ratio was held constant, using amounts of purified MAPs above those previously determined to saturate binding to the microtubule lattice (Cleveland et al., 1977; Kim et al., 1979). For the following reasons, our observations were limited to a range of tubulin concentrations between 4 and 9 μM. In general, MAPs promote microtubule assembly at lower tubulin concentrations than occurs for MAP-free tubulin (see Fig. 3). In the presence of MAPs, nucleation occurs at tubulin concentrations above 4 μM. This threshold contrasts with that for pure tubulin, which does not undergo frequent nucleation below about 7 μM (Walker et al., 1988). For MAP-containing microtubules, accurate transition frequency data could not be obtained at tubulin concentrations above 9 μM because most microtubule ends elongated beyond the microscope's field of view without undergoing catastrophe. Therefore, our analysis of the dynamic instability of MAP-containing microtubules is limited by nucleation to 4 μM as the lowest tubulin concentration and by catastrophe to 9 μM as the highest tubulin concentration observable.

Both the plus and minus ends of microtubules assembled in the presence of hs MAP, MAP2 or tau exhibited characteristic features of dynamic instability (Figs 1 and 2) at the tubulin concentrations used in this study. Fig. 1 shows an example of microtubule dynamic instability in the presence of purified tau. All microtubules grew at constant rates during the elongation phase. Transitions from the elongation phase to rapid shortening (catastrophe) were abrupt and stochastic (Fig. 1; 10 s). A rapidly shortening microtubule either shortened until it disappeared, or was rescued after a variable length of time (Fig. 1; 40 s). Rescue, the transition from rapid shortening to elongation, was also abrupt and appeared to be stochastic. After rescue, a microtubule resumed the elongation phase (Fig. 1; 50 s to 1:50) for a length of time unrelated to the length of the previous phase, and elongated until the next catastrophe.

Representative examples of the dynamic histories of individual plus and minus ends of microtubules in the presence of saturating amounts of MAP2 and tau are shown in Fig. 2. Dynamic histories of microtubules assembled from purified tubulin at the same tubulin concentrations are plotted for comparison (Walker et al., 1988). Microtubules assembled with hs MAPs exhibited similar dynamic instability behavior, but only at very low tubulin concentrations, as discussed below. The duration of the shortening phase of the microtubule assembled with tau in Fig. 2a is longer than the average for tau-containing microtubules at this tubulin concentration, and was chosen to illustrate the extensive shortening possible for microtubules when MAPs are bound to the microtubule lattice. When compared to microtubules assembled from purified tubulin, microtubules assembled in the presence of each MAP preparation used in this study elongated at faster rates, shortened at only slightly slower rates, and exhibited fewer catastrophes and more rescues.

*MAPs increase the rate of microtubule elongation by decreasing tubulin dissociation during elongation*

Average rates of elongation plotted as a function of active tubulin concentration in the presence of each MAP preparation are shown in Fig. 3. Data for MAP-free microtubules (using the same tubulin preparations; Walker et al., 1988) are also given for comparison. All three MAP preparations increased the average rate of elongation for both the plus and minus ends. Both hs MAPs and the purified brain MAPs had little or no effect on the apparent association rate constants for the plus and minus ends (as determined from the slope of a line drawn through the MAP-microtubule data points). However, all the MAP preparations decreased the apparent tubulin dissociation rate constant during elongation (*x*-intercept of the line drawn through the MAP-microtubule data points). This lowered the critical concentration for elongation ($S_c^e$; the concentration needed for net

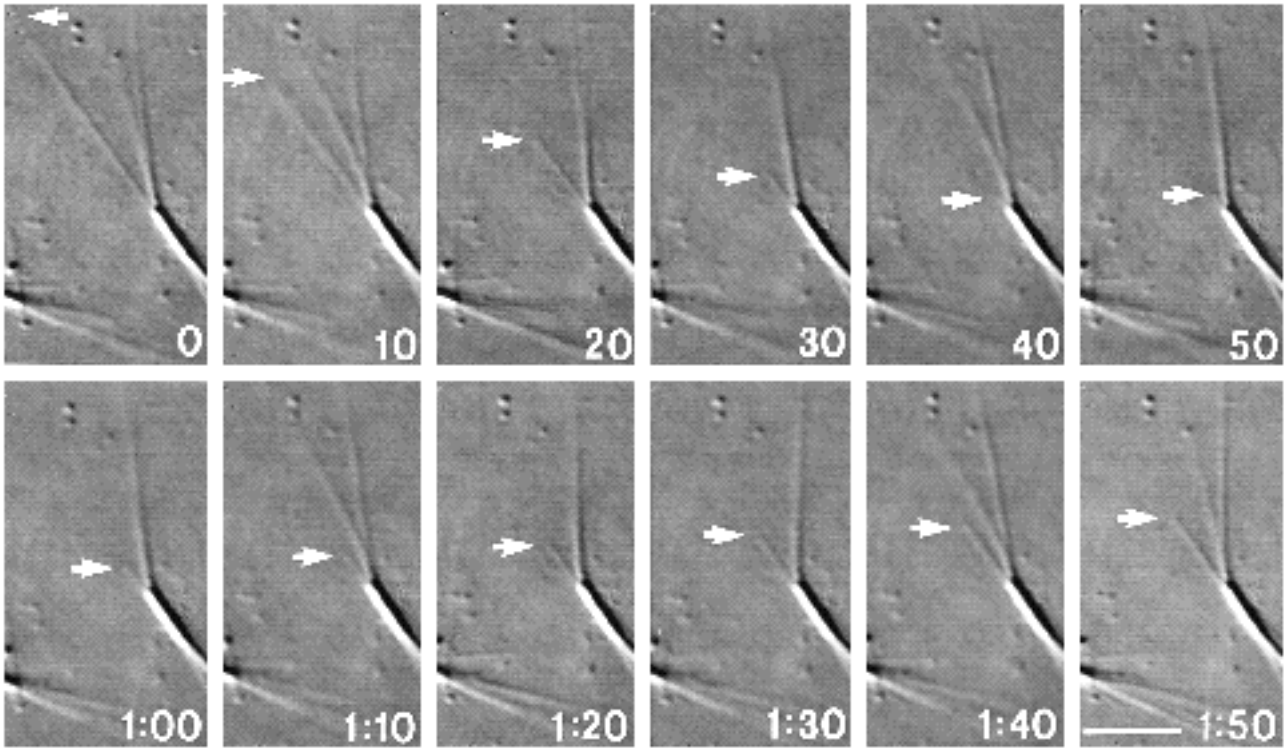


**Fig. 1.** A series of micrographs taken from a real-time video recording of microtubules undergoing dynamic instability. Microtubules assembled from 9 μM tubulin in the presence of 4.5 μM tau were nucleated by axoneme fragments and elongated from both ends of the axoneme. One plus end microtubule (marked with an arrow) underwent a catastrophe between 0 and 10 s and began rapid shortening. At 40 s, the shortening microtubule was rescued, and resumed elongation. The extent of the rapid shortening phase shown for this microtubule is longer than average for tau-containing microtubules at this tubulin concentration. This dynamic behavior is also presented as a life history plot in Fig. 2a. Time is shown in minutes and seconds. Bar, 5 μm.

elongation) from about 5 μM for pure tubulin to about 1 μM or less in the presence of MAPs.

*MAPs decrease the catastrophe frequency*

Catastrophes of MAP-containing microtubules were stochastic and not preceded by a change in the elongation rate. All of the MAP preparations decreased the frequency of catastrophe of both plus and minus end microtubules below the values expected for MAP-free microtubules at any given concentration of tubulin, as shown in Fig. 4a. Fig. 4a also includes catastrophe frequencies of microtubules composed of purified tubulin from studies of spontaneous catastrophe (Walker et al., 1988) and dilution studies of catastrophe frequencies at lower tubulin concentrations (Walker et al., 1991). Heat-stable MAPs (triangles, Fig. 4a) dramatically decreased the catastrophe frequency, and above 6 μM tubulin catastrophes were not detected for either plus or minus ends during observation periods as long as 112 minutes (for 6 μM tubulin, plus end). Below 5 μM tubulin, in the presence of hs MAPs, catastrophe frequencies were greatly decreased in comparison with the expected frequencies for pure tubulin. In contrast to the hs MAPs, catastrophes were observed at higher tubulin concentrations (7-9 μM) in the presence of purified tau and MAP2, but still occurred less often than for MAP-free microtubules. The frequency of catastrophe for MAP-free microtubules has been shown to decrease with increasing tubulin concentration (Walker et al., 1988; O'Brien et al., 1990; Walker et al., 1991). Catastrophe in the presence of MAPs was less frequent at higher tubulin concentration, but the exact relationship could not be established within the limited range of tubulin concentrations studied.

*MAPs decrease the rate, but do not block, rapid shortening*

Although the MAP fractions we assayed decreased the catastrophe frequency, they only decreased the average rates of rapid shortening by about 50% from the rates observed for microtubules assembled in the absence of MAPs (Table 1). Average rates of rapid shortening for microtubules assembled from purified tubulin are independent of tubulin concentration over a range of 0 to 25 μM (Walker et al., 1988; Walker et al., 1989). We also found that rapid shortening rates in the presence of MAPs were not dependent on tubulin concentration, and the data in Table 1 are presented as average rates for all tubulin concentrations and each MAP preparation. Following spontaneous catastrophe, microtubules shortened at constant velocity until rescue occurred or the microtubule completely depolymerized. Averaged over the total population of microtubules, the measured rates of shortening in the presence of MAPs are slower than for pure tubulin alone. However, the velocity of shortening at either end varied substantially between different microtubules under the same conditions, as seen by the high values for standard deviation in Table 1. As a result

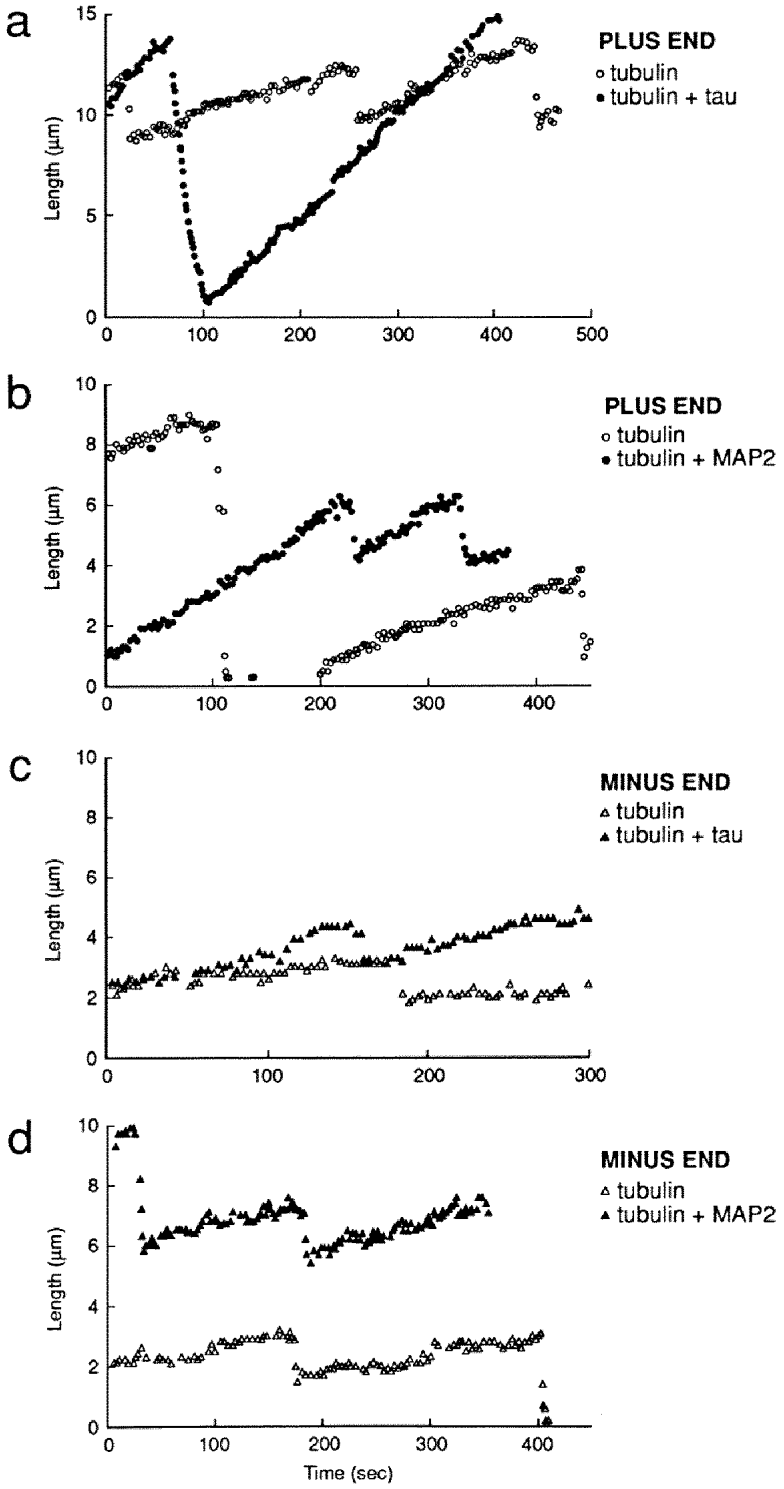


**Fig. 2**. Representative examples of life histories of MAP-free and MAP-containing microtubules. Plots were generated by tracking the position of the microtubule end in real-time video recordings. Each plot compares MAP-free and MAP-containing microtubules of the same polarity at a similar tubulin concentration. (a) (●)Plus end, 9 μM tubulin + 4.5 μM tau MAPs; (○) plus end, 10 μM purified tubulin. (b) (●) Plus end, 7.5 μM tubulin + 0.95 μM MAP2; (○) plus end, 8.7 μM tubulin. (c) (▲) Minus end, 7 μM tubulin + 3.5 μM tau MAPs; (△) minus end, 6.8 μM tubulin. (d) (▲) Minus end, 7.5 μM tubulin + 0.95 μM MAP2; (△) minus end, 6.8 μM tubulin.

of this high variation between microtubules, the rapid shortening rates of microtubules in the presence of MAP2 or tau were not significantly different from those of MAP-free microtubules ($P<0.001$; independent *t*-test of plus or minus polarity MAP-free microtubules versus plus or minus polarity microtubules assembled with tau or MAP2).

One concern about the rates of spontaneous rapid shortening in the presence of MAPs was that the relatively fast shortening rates might be due to heterogeneous MAP distribution along microtubules. Rapid shortening might be explained by shortening in regions at the tip of the microtubule depleted of MAPs, and rescue might occur when rapid shortening reached a MAP-rich region of the microtubule. To address this possibility, we used a perfusion chamber to initially assemble microtubules in the presence of MAPs. The chamber was then perfused with a solution containing MAP2, but not tubulin, to promote catastrophe while maintaining constant MAP2 concentration (Walker et

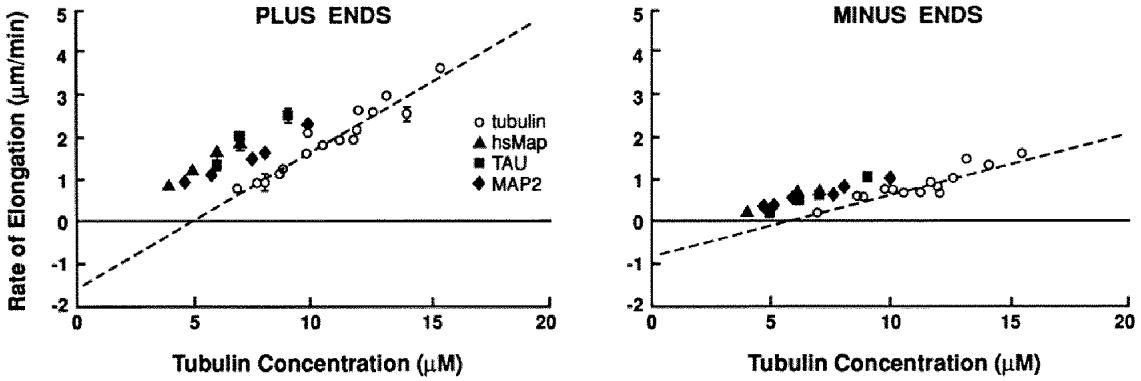


**Fig. 3.** Rates of elongation of plus and minus microtubule ends, plotted as a function of tubulin subunit concentration. Each point represents the mean elongation rate (*n*=average of 22 microtubules per data point) in the presence of each of three MAP preparations: (▲) heat-stable MAPs; (■) tau; (◆) MAP2. Data for MAP-free microtubules from the same tubulin preparations (Walker et al., 1988) are plotted for comparison (○) on each plot, and regression line). Error bars represent s.e.m.

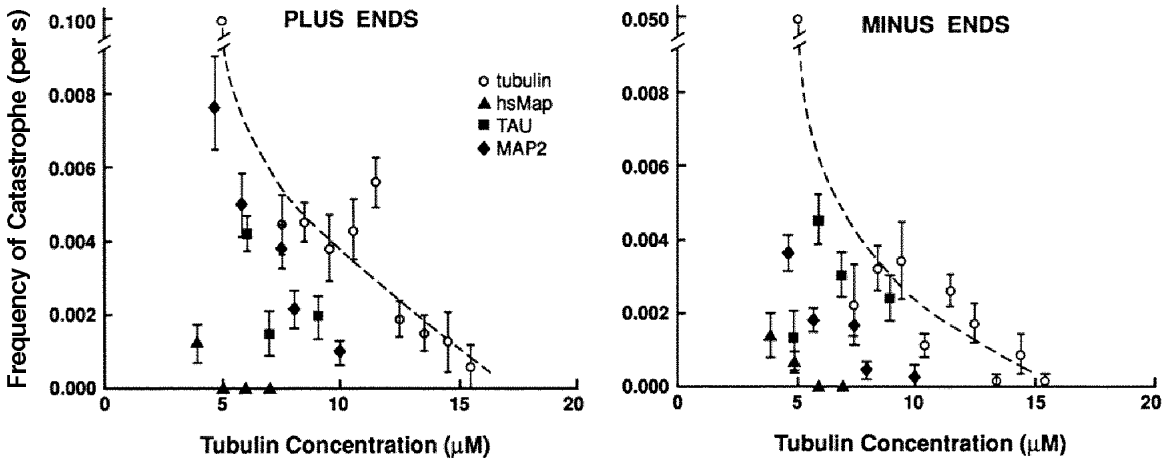


**Fig. 4.** Frequency of catastrophe of plus and minus microtuble ends, plotted as a function of tubulin subunit concentration: (▲) heat-stable MAPs; (■) tau; (◆) MAP2. Catastrophe frequencies for MAP-free microtubules from the same tubulin preparations (Walker et al., 1988) are shown for comparison (○). Catastrophe frequency for purified tubulin at 4.5 μM is taken from the dilution studies of Walker et al. (1991). This method for determining $k_c$ yields values similar to those determined from steady-state measurements (O'Brien et al., 1990; Walker et al., 1991). Error bars represent standard deviations, calculated as $k_c/(n)$. *n*=average of 22 microtubules per data point.

al., 1991). The MAP2 perfusion buffer maintained MAP2 at the same concentration (1 μM) used to promote tubulin assembly, but the free tubulin concentration was diluted rapidly to below 3 μM. Upon dilution, microtubules converted to the rapid shortening phase within several seconds following dilution, and shortened completely back to the nucleation site (Pryer, 1989), as occurred following dilution of microtubules assembled from pure tubulin and diluted by perfusion with buffer alone (Walker et al., 1991). For either plus or minus ends, the average shortening rates following dilution were typical of the rates measured for spontaneous shortening in the presence and absence of MAP2 (Table 1), as expected if MAPs were bound uniformly along the length of a microtubule. Following dilution-induced catastrophe, about 15% of microtubules observed paused during shortening for an average of 1.1 seconds.

*MAPs increase the frequency of rescue, but extensive shortening prior to rescue can occur with MAP2 or tau*

In addition to decreasing the frequency with which microtubules convert to the rapid shortening phase, each MAP preparation generally decreased the average time spent in the shortening phase by increasing the frequency of rescue (Fig. 5). The hs MAPs and MAP2 increased the frequency of rescue for both plus and minus microtubule ends, while rescue frequencies for tau-containing microtubules were generally lower than for the other MAPs. We have previously shown that the frequency of rescue at the minus end was steeply concentration-dependent for MAP-free microtubules (Walker et al., 1988). In the present study, neither MAP2- nor tau-containing microtubules appeared to exhibit this concentration dependence at the low tubulin concentrations used. This may be due to the difficulty of determining concentration dependence over a limited range of tubulin concentrations. As for microtubules assembled from purified tubulin, the frequency of rescue at the minus end

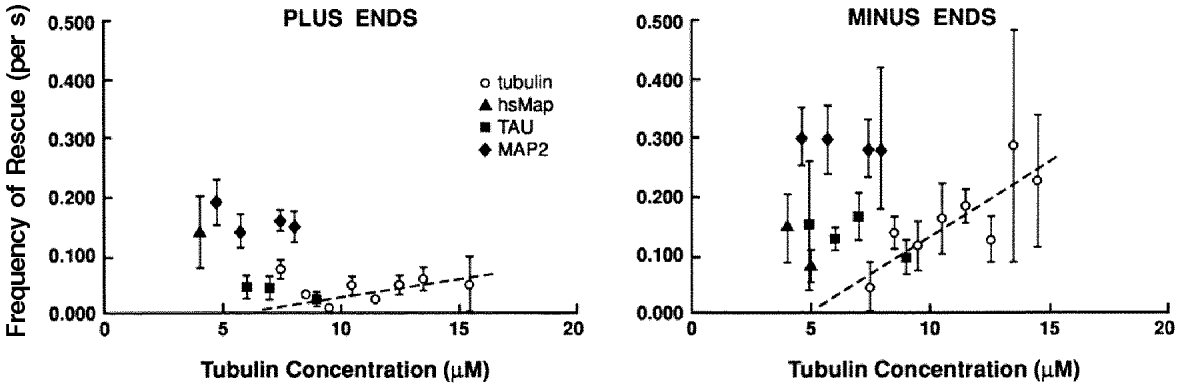


**Fig. 5.** Frequency of rescue of plus and minus microtuble ends, plotted as a function of tubulin subunit concentration: (▲) heat-stable MAPs; (■) tau; (◆) MAP2. Rescue frequencies for MAP-free microtubules from the same tubulin preparations (Walker et al., 1988) are shown for comparison (○). Error bars represent standard deviations, calculated as $k_r/(n)$. *n*=average of 22 microtubules per data point.

**Table 1.** *Rates of shortening for MAP-free and MAP-containing microtubules*

| | Plus ends | | Minus ends | |
|---|---|---|---|---|
| | (μm/min ± s.d.) | (*n*) | (μm/min ± s.d.) | (*n*) |
| Purified tubulin* | 26.9 ± 10.8 | (166) | 34.0 ± 16.7 | (41) |
| Pure tubulin dilution | 32.0 ± 13.3 | (18) | 47.2 ± 21.0 | (12) |
| + hs MAPs† | 12.6 ± 9.8 | (5) | 13.5 ± 13.7 | (13) |
| + tau‡ | 14.9 ± 6.5 | (18) | 22.9 ± 17.8 | (87) |
| + MAP2‡ | 22.8 ± 15 | (120) | 22.9 ± 15.8 | (99) |
| + MAP2 dilution§ | 13.1 ± 9.6 | (10) | 26.3 ± 15.6 | (8) |

*Measured over the range of 7.0-15.5 μM tubulin.

†Few rapid shortening events were observed, and only at 4 μM and 5 μM tubulin.

‡Measured over the range of 6-9 μM tubulin for tau and 5-8 μM tubulin for MAP2.

§Assembled MAP2-microtubules were perfused with PM buffer containing 1 μM MAP2.

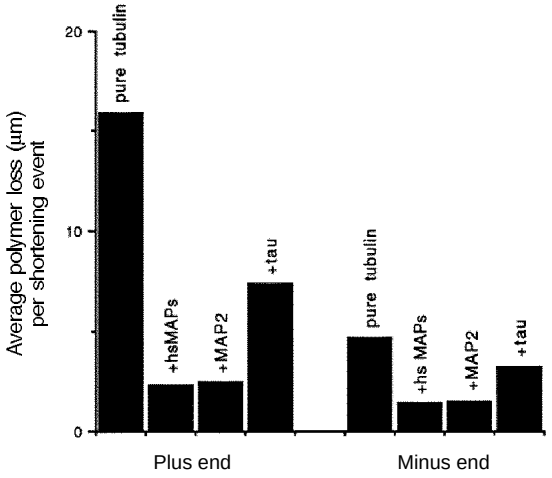


**Fig. 6.** Average microtubule polymer loss per rapid shortening event, calculated as $1/k_c \cdot V_{shortening}$, summed for all microtubules of each MAP preparation and each polarity.

in the presence of MAPs was higher than for plus ends. Rescue has not been observed for microtubules assembled from pure tubulin at concentrations below the critical concentration for elongation (5 μM tubulin) (Walker et al., 1988; Walker et al., 1989). For microtubules assembled with MAPs, rescues were observed at tubulin concentrations as low as 3 μM (Fig. 5). This result correlates with the lower critical concentration for elongation in the presence of MAPs (Fig. 3).

Although the rescue frequency was higher for the MAP-containing microtubules in this study than for microtubules composed of pure tubulin, the durations of shortening phases were still long enough to permit the loss of considerable polymer length. We estimated the average amount of polymer lost during each rapid shortening phase as product of the inverse of the rescue frequency and the average rate of rapid shortening. Since rescue frequency and rapid shortening rates did not vary with tubulin concentration, average polymer loss was determined by summing the data for all tubulin concentrations for each MAP preparation. These calculations indicated a greater loss of polymer from the plus end, in accordance with the lower frequency of rescue at the plus end (Fig. 6). For example, microtubules assembled with purified tau lost an average of 7.4 μm (12,000 dimers) per rapid shortening event at the plus end, and 3.2 μm (5250 dimers) per rapid shortening event at the minus end, as reflected in the lower rescue frequencies for tau-containing microtubules.

## Discussion

We have shown that the mammalian brain heat-stable MAP fraction, MAP2, and tau promote microtubule assembly by promoting nucleation, blocking tubulin subunit dissociation during the elongation phase, decreasing catastrophe frequency, slowing tubulin dissociation during the shortening phase and enhancing the rescue frequency. Purified MAP2 and tau, used in amounts previously determined to saturate binding sites along the microtubule lattice, had quantitatively similar effects to those of the hs MAPs on elongation and shortening velocities at either plus or minus microtubule ends. However, the hs MAPs produced much more stable microtubules than either MAP2 or tau by inhibiting

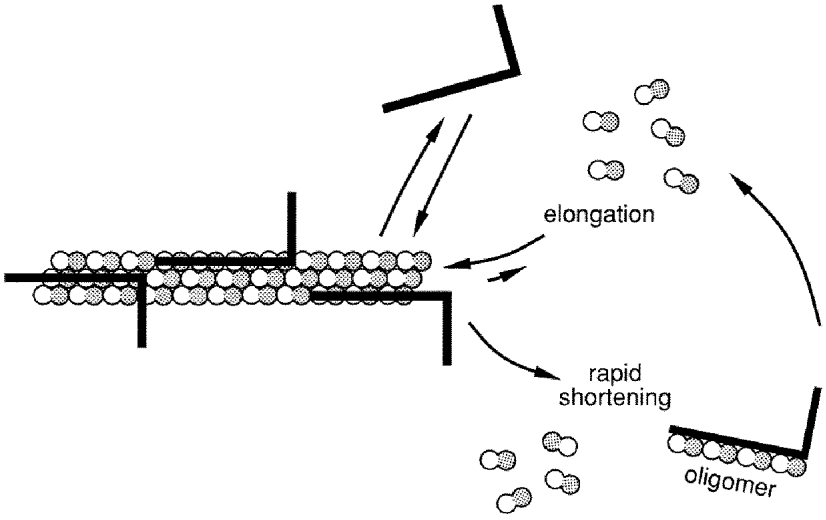


**Fig. 7.** Model of elongation and rapid shortening in the presence of MAPs, as discussed in text. Only three protofilaments are drawn. Tubulin dimers are represented as dumbbell shapes; MAPs are drawn as large L-shaped molecules.

catastrophe at all but the lowest tubulin concentrations (4-5 μM) assayed in our study. The stability of microtubules in the presence of the hs MAP fraction resembles the stability reported previously for microtubules assembled with unfractionated brain MAPs (Sloboda et al., 1976; Murphy et al., 1977; Bergen and Borisy, 1980). We do not know whether the suppression of catastrophe that we observed in the presence of hs MAPs is produced by interactions between MAP2 and tau in that fraction, or by another factor in the hs MAP fraction. It would be interesting to fractionate the hsMAPs in order to identify the stabilizing activity present in this preparation. It is clear from our kinetic data that if the tubulin concentration is sufficiently low, frequent catastrophe and extensive shortening can occur for microtubules in the presence of either hs MAPs, MAP2 or tau. Thus, none of these MAP fractions abolishes the fundamental mechanism of dynamic instability inherent in the tubulin lattice of the microtubule. The MAPs we studied only modulate the rate constants and transition frequencies of dynamic instability.

The hs MAPs, tau and MAP2 all increased the net elongation rate at both microtubule ends. MAPs did not substantially decrease the dimer association rate above the values for pure tubulin. Instead, all the MAPs we studied stabilized the incorporation of newly bound tubulin dimers into the microtubule lattice, increasing the net elongation rate of the microtubule. Similar effects have been reported for unfractionated brain MAPs, based upon spectrophotometric measurements of initial rates of assembly of three-cycled microtubule protein (Murphy et al., 1977). The decrease in dimer dissociation rate during elongation produced by MAPs yields a lower critical concentration for elongation, consistent with previously determined values for critical concentration in the presence of MAPs, which range from 0.5 μM to 3.5 μM (Cleveland et al., 1977; Kim et al., 1979; Sloboda and Rosenbaum, 1979; Farrell et al., 1987). The effect of MAPs on the dimer dissociation rate during elongation may also provide an explanation for the more frequent nucleation events observed at low tubulin concentrations in comparison with assembly from purified tubulin.

Microtubules in the presence of MAPs tended to persist longer than those assembled from purified tubulin, mainly because MAPs decreased catastrophe frequency and increased rescue frequency. Despite the increase in polymer stability, we found that rapid shortening can still be extensive in the presence of both purified MAP2 or tau. For example, the plus end of tau-containing microtubules lost an average of 7 μm (about 12,000 dimers) in each rapid shortening event. Although tau and MAP2 appear to share common binding sites on the microtubule lattice (Sandoval and Vandekerckhove, 1981; Littauer et al., 1986), the rescue data (Fig. 5) show that MAP2 is more effective than tau at promoting rescue.

How then can MAP2 or tau interact independently with the microtubule lattice to increase the elongation rate and decrease the frequency of catastrophe, and yet allow extensive rapid shortening events to occur? One possibility is that rapid shortening occurs in our experiments only over regions of the microtubule having low concentrations of MAPs (Job et al., 1985). This possibility is unlikely for several reasons. In our studies, we used MAPs in amounts well above those necessary to saturate all the binding sites along all microtubules in our preparations. This should have prevented a heterogeneous MAP distribution, since electron microscopy studies of microtubules in vitro show that MAP binding sites are distributed evenly along the length of the microtubules (Murphy and Borisy, 1975; Sloboda et al., 1976; Kim et al., 1979). Consistent with a homogeneous distribution of MAPs along the length of the microtubule, no fluctuations in the velocity of elongation were observed. Microtubule elongation was constant at the ends of microtubules until a catastrophe occurred. As a direct test for heterogeneous MAP stabilization, we measured the kinetics of rapid shortening of MAP-containing microtubules upon dilution of the tubulin subunit concentration in the presence of MAP2 (Pryer, 1989). All microtubules rapidly shortened at rates similar to those reported for spontaneous shortening.

A model to explain microtubule dynamics in the presence of MAP2 or tau is presented in Fig. 7. In this model, tau or MAP2 binds primarily to sites along protofilaments, stabilizing the addition of single tubulin dimers to the microtubule end during elongation. tau or MAP2 strength-

ens the longitudinal bonds between tubulin dimers within protofilaments, reducing the rate of tubulin dissociation during elongation. In this model, saturating amounts of MAP2 or tau alone have comparatively little effect on the strength of lateral interactions between tubulin dimers in adjacent protofilaments. Thus subunit dissociation during the shortening phase still occurs at rates of similar magnitude to rapid shortening in the absence of MAPs. When catastrophe occurs, shortening proceeds by the loss of oligomers of MAP-bound tubulin subunits. Several studies support the formation of transient oligomers generated from protofilaments during disassembly of MAP-containing microtubules (Mandelkow et al., 1988; Melki et al., 1988; Simon and Salmon, 1990; Mandelkow et al., 1991). The number of dimers constituting an oligomer is not known, nor is the exact size of the microtubule binding domain of MAPs.

The molecular mechanisms of catastrophe and rescue in MAP-containing microtubules must be a function of both MAP binding characteristics and the underlying dynamic behavior intrinsic to pure tubulin. The dynamic instability behavior of microtubules assembled from purified tubulin is thought to be regulated by a stable tubulin cap that is constrained to the tip of elongating microtubules (O'Brien et al., 1987; Stewart et al., 1990; Walker et al., 1991). It is not clear whether stabilization by this cap is due to the chemical nature of the terminal subunits (i.e. GTP vs GDP), the conformational nature of the subunits, or some combination of the two (for review, see Caplow, 1992). In our model (Fig. 7), MAPs decrease catastrophe frequency by inhibiting the dissociation of stable tubulin subunits from the cap. In addition, MAPs may also suppress a conformational change in the lattice that is needed for a microtubule end to convert to the shortening phase (Walker et al., 1989; Stewart et al., 1990). Perhaps the strong suppression of catastrophe by the hs MAP fraction can be explained by a stronger stabilization of lattice conformation by the hs MAPs in comparison to purified tau or MAP2 alone. Rescue is thought to be due to 'recapping' a shortening microtubule by adding GTP-tubulin dimers sufficient to stabilize the GDP core (Mitchison and Kirschner, 1984a; Walker et al., 1988). In our model, the brain MAPs enhance rescue by increasing the probability of successfully incorporating GTP-tubulin subunits onto GDP-tubulin subunits at the shortening microtubule end. Our rescue data indicate that the hs MAPs were most effective at promoting rescue, while tau was least effective.

Microtubules in differentiated (post-mitotic) neurons appear to be more stable than cytoplasmic microtubules of mitotically active cells. Consistent with a role in stabilizing extended axons (Daniels, 1972), and serving as stable tracks for vesicular transport in the axon (Grafstein and Forman, 1980), neuronal microtubules are relatively resistant to depolymerization by colcemid (Bamburg et al., 1986), incorporate tubulin subunits slowly (Okabe and Hirokawa, 1988), and exhibit infrequent rapid shorting events in vitro (Seitz-Tutter et al., 1988). This suppression of dynamic instability is similar to that exhibited in the presence of hs MAPs in our study and unfractionated MAPs in other studies (Horio and Hotani, 1986; Farrell et al., 1987; Hotani and Horio, 1988). Neither MAP2 nor tau suppressed dynamic instability to the extent that occurred for hs MAPs in vitro or for microtubules in living axons. MAP2 and tau are not expressed in non-neuronal cells, but these MAPs have been microinjected into living non-neuronal cells to study their effects on more dynamic microtubules in these tissue cells. Microinjected tau and MAP2 both promoted microtubule assembly and stability, but to different extents. tau appears to decrease substantially the rate at which microtubules convert to the rapid shortening phase in response to the microtubule-depolymerizing agent nocodazole (Drubin and Kirschner, 1986). However, microinjected MAP2 did not appear to stabilize microtubules against nocodazole-induced depolymerization (Olmsted et al., 1989). MAP2 and tau alone do not bundle microtubules in vitro, but both have been observed to bundle microtubules when expressed by DNA transfection in tissue culture cells (Kanai et al., 1989; Lewis et al., 1989), suggesting that in the cell, the MAPs associate with other cellular components, enhancing microtubule stability by bundling (Tanaka and Kirschner, 1991). Our results predict that neurons and non-neuronal cells both contain factors that can bind to MAP2 or tau and substantially enhance their stabilization of microtubule dynamics.

The most striking difference between the assembly dynamics of the brain MAP-containing microtubules seen in our studies and the dynamic instability of microtubules in interphase tissue cells is in the frequency of catastrophe. At cellular tubulin concentrations of 10-20 μM (Hiller and Weber, 1978), microtubules elongate at 5-15 μm/min (Schulze and Kirschner, 1986; Cassimeris et al., 1988; Sammak and Borisy, 1988; Belmont et al., 1990; Simon and Salmon, 1990; Glicksman et al., 1992). These velocities are similar to projected elongation rates in the presence of brain MAPs, at equivalent tubulin concentrations (see Fig. 3). However, in the presence of brain MAPs at these tubulin concentrations, catastrophe would be rare (Fig. 4). In contrast, for the majority of microtubule plus ends in interphase non-neuronal cells, a catastrophe occurs on average once every 50 seconds of elongation ($k_c$ = 0.02 $s^{-1}$) (Cassimeris et al., 1988; Belmont et al., 1990; Simon and Salmon, 1990; Glicksman et al., 1992). This 100-fold or more difference in catastrophe frequency at similar growth velocity could be due to differences in solution conditions in vitro (Simon and Salmon, 1992). It is more likely that other factors such as post-translational modifications of MAPs affect cellular microtubule dynamics. For example, the phosphorylation state of MAP2 affects the affinity of MAP2 for the microtubule lattice and the degree of stimulation of microtubule assembly by MAP2 (Jameson and Caplow, 1981; Murthy and Flavin, 1983; Burns et al., 1984; Brugg and Matus, 1991). Cells might also contain additional factors that specifically promote catastrophe by interacting with elongating microtubule ends (Simon and Salmon, 1990; Walker et al., 1991). Different types of MAPs are found in different cell and tissue types, as well as in different species (Vallee and Bloom, 1984; Olmsted, 1986), so that requirements for relatively stable or dynamic microtubules might be conferred by MAPs specific to certain cells or tissues. More intensive studies of a variety of non-neuronal MAPs are needed to discover the range of

effects that different types of MAPs exert on microtubule dynamics.

We thank Lynne Cassimeris, Harold Erickson, Michael Caplow, Tim O'Brien and Doug Murphy for valuable discussions and/or critical reading of the manuscript. We are grateful for the computer programming expertise of Steve Magers, and invaluable assistance in figure preparation from Susan Whitfield. This work was supported by NIH GM 24364 and NSF DCB-8616621.

## References

**Bamburg, J. R., Bray, D. and Chapman, K.** (1986). Assembly of microtubules at the tip of growing axons. *Nature* **321**, 788-780.

**Bell, C. W., Fraser, C., Sale, W. S., Tang, W.-J. Y. and Gibbons, I. R.** (1982). Preparation and purification of dynein. *Meth. Cell Biol*. **24**, 373-397.

**Belmont, L. D., Hyman, A. A., Sawin, K. E. and Mitchison, T. J.** (1990). Real-time visualization of cell cycle-dependent changes in microtubule dynamics in cytoplasmic extracts. *Cell* **62**, 579-589.

**Berg, H. C. and Block, S. M.** (1984). A miniature flow cell designed for rapid exchange of media under high-power microscope objectives. *J. Gen. Microbiol.* **130**, 2915-2920.

**Bergen, L. G. and Borisy, G. G.** (1980). Head-to-tail polymerization of microtubules in vitro. *J. Cell Biol.* **84**, 141-150.

**Bre, M. H. and Karsenti, E.** (1990). Effects of brain microtubule-associated proteins on microtubule dynamics and the nucleating activity of centrosomes. *Cell Motil. Cytoskel.* **15**, 88-98.

**Brugg, B. and Matus, A.** (1991). Phosphorylation determines the binding of microtubule-associated protein 2 (MAP2) to microtubules in living cells. *J. Cell Biol.* **114**, 735-743.

**Burns, R. G., Islam, K. and Chapman, R.** (1984). The multiple phosphorylation of the microtubule-associated protein MAP2 controls the MAP2:tubulin interaction. *Eur. J. Biochem.* **141**, 609-615.

**Caplow, M.** (1992). Microtubule dynamics. *Curr. Opin. Cell Biol.* **4**, 58-65.

**Cassimeris, L., Pryer, N. K. and Salmon, E. D.** (1988). Real-time observations of microtubule dynamic instability in living cells. *J. Cell Biol.* **107**, 2223-2231.

**Cassimeris, L. U., Walker, R. A., Pryer, N. K. and Salmon, E. D.** (1987). Dynamic instability of microtubules. *Bioessays* **7**, 149-154.

**Cleveland, D. W., Hwo, S.-Y. and Kirschner, M. W.** (1977). Purification of tau, a microtubule-associated protein that induces assembly of microtubules from purified tubulin. *J. Mol. Biol.* **116**, 207-225.

**Daniels, M. P.** (1972). Colchicine inhibition of nerve fiber formation in vitro. *J. Cell Biol.* **53**, 164-176.

**Drubin, D. G. and Kirschner, M. W.** (1986). Tau protein function in living cells. *J. Cell Biol.* **103**, 2739-2746.

**Farrell, K. W., Jordan, M. A., Miller, H. P. and Wilson, L.** (1987). Phase dynamics at microtubule ends: the coexistence of microtubule length changes and treadmilling. *J. Cell Biol.* **104**, 1035-1046.

**Glicksman, N. R., Parsons, S. F. and Salmon, E. D.** (1992). Okadaic acid induces interphase to mitotic-like microtubule dynamic instability by inactivating rescue. *J. Cell Biol.* (in press).

**Grafstein, B. and Forman, D. S.** (1980). Intracellular transport in neurons. *Physiol. Rev.* **60**, 1167-1283.

**Hiller, G. and Weber, K.** (1978). Radioimmune assay for tubulin: A quantitative comparison of the tubulin content of different established tissue culture cells and tissues. *Cell* **14**, 795-804.

**Hirokawa, N., Shiomura, Y. and Okabe, S.** (1988). Tau proteins: The molecular structure and mode of binding on microtubules. *J. Cell Biol.* **107**, 1449-1459.

**Horio, T. and Hotani, H.** (1986). Visualization of the dynamic instability of individual microtubules by dark-field microscopy. *Nature* **321**, 605-607.

**Hotani, H. and Horio, T.** (1988). Dynamics of microtubules visualized by darkfield microscopy: treadmilling and dynamic instability. *Cell Motil. Cytoskel.* **10**, 229-236.

**Jameson, L. and Caplow, M.** (1981). Modification of microtubule steady-state dynamics by phosphorylation of the microtubule-associated proteins. *Proc. Nat. Acad. Sci. U.S.A.* **78**, 3413-3417.

**Job, D., Pabion, M. and Margolis, R. M.** (1985). Generation of microtubule stability subclasses by microtubule-associated proteins: implications for the microtubule "dynamic instability" model. *J. Cell Biol.* **101**, 1680-1689.

**Kanai, Y., Takemura, R., Oshima, T., Mori, H., Ihara, Y., Yanagisawa, M., Masaki, T. and Hirokawa, N.** (1989). Expression of multiple tau isoforms and microtubule bundle formation in fibroblasts transfected with a single cDNA clone. *J. Cell Biol.* **109**, 1173-1184.

**Kim, H., Binder, L. I. and Rosenbaum, J. L.** (1979). The periodic association of MAP 2 with brain microtubules in vitro. *J. Cell Biol.* **80**, 266-276.

**Lewis, S. A., Ivanov, I. E., Lee, G.-H. and Cowan, N. J.** (1989). Organization of microtubules in dendrites and axons is determined by a short hydrophobic zipper in microtubule-associated proteins MAP2 and tau. *Nature* **342**, 498-505.

**Lewis, S. A., Wang, D. and Cowan, N. J.** (1988). Microtubule-associated protein MAP2 shares a microtubule binding motif with tau protein. *Science* **242**, 936-939.

**Littauer, U. Z., Giveon, D., Thierauf, M., Ginzburg, I. and Ponstingl, H.** (1986). Common and distinct tubulin binding sites for microtubule-associated proteins. *Proc. Nat. Acad. Sci. U.S.A.* **83**, 7162-7166.

**Lutz, D. A. and Inoue, S.** (1986). Techniques for observing living gametes and embryos. *Meth. Cell Biol.* **27**, 89-110.

**Mandelkow, E.-M., Lange, G., Jagla, A., Spann, U. and Mandelkow, E.** (1988). Dynamics of the microtubule oscillator: role of nucleotides and tubulin-MAP interactions. *EMBO J.* **7**, 357-365.

**Mandelkow, E.-M., Mandelkow, E. and Milligan, R. A.** (1991). Microtubule dynamics and microtubule caps: a time-resolved cryoelectron microscopy study. *J. Cell Biol.* **114**, 977-991.

**Melki, R., Carlier, M.-F. and Pantaloni, D.** (1988). Oscillations in microtubule polymerization: the rate of GTP regeneration on tubulin controls the period. *EMBO J.* **7**, 2653-2659.

**Mitchison, T. and Kirschner, M.** (1984a). Dynamic instability of microtubule growth. *Nature* **312**, 237-242.

**Mitchison, T. and Kirschner, M.** (1984b). Microtubule assembly nucleated by isolated centrosomes. *Nature* **312**, 232-237.

**Murphy, D. B. and Borisy, G. G.** (1975). Association of high-molecular-weight proteins with microtubules and their role in microtubule assembly in vitro. *Proc. Nat. Acad. Sci. U.S.A.* **72**, 2696-2700.

**Murphy, D. B., Johnson, K. A. and Borisy, G. G.** (1977). Role of tubulin-associated proteins in microtubule nucleation and elongation. *J. Mol. Biol.* **117**, 33-52.

**Murphy, D. B., Vallee, R. B. and Borisy, G. G.** (1977). Identity and polymerization-stimulatory activity of the non-tubulin proteins associated with microtubules. *Biochemistry* **16**, 2598-2605.

**Murthy, A. S. and Flavin, M.** (1983). Microtubule assembly using microtubule-associated protein MAP2 prepared in defined states of phosphorylation with protein kinase and phosphatase. *Eur. J. Biochem.* **137**, 37-46.

**O'Brien, E. T., Salmon, E. D., Walker, R. A. and Erickson, H. P.** (1990). Effects of magnesium on the dynamic instability of individual microtubules. *Biochemistry* **29**, 6648-6656.

**O'Brien, E. T., Voter, W. A. and Erickson, H. P.** (1987). GTP hydrolysis during microtubule assembly. *Biochemistry* **26**, 4148-4156.

**Okabe, S. and Hirokawa, N.** (1988). Microtubule dynamics in nerve cells: analysis using microinjection of biotinylated tubulin into PC12 cells. *J. Cell Biol.* **107**, 651-664.

**Olmsted, J. B.** (1986). Microtubule-associated proteins. *Annu. Rev. Cell Biol.* **2**, 421-457.

**Olmsted, J. B., Stemple, D. L., Saxton, W. M., Neighbors, B. W. and McIntosh, J. R.** (1989). Cell cycle-dependent changes in the dynamics of MAP2 and MAP4 in cultured cells. *J. Cell Biol.* **109**, 211-223.

**Pryer, N. K.** (1989). Individual microtubule dynamics observed by video microscopy. Ph.D. thesis, University of North Carolina, Chapel Hill.

**Pryer, N. K., Wadsworth, P. and Salmon, E. D.** (1986). Polarized microtubule gliding and particle saltations produced by soluble factors from sea urchin eggs and embryos. *Cell Motil. Cytoskel.* **6**, 537-548.

**Salmon, E. D., Walker, R. A. and Pryer, N. K.** (1989). Video-enhanced differential interference contrast light microscopy. *BioTechniques* **7**, 624-633.

**Sammak, P. J. and Borisy, G. G.** (1988). Direct observation of microtubule dynamics in living cells. *Nature* **332**, 724-726.

**Sandoval, I. V. and Vandekerckhove, J. S.** (1981). A comparative study of the in vitro polymerization of tubulin in the presence of the microtubule-associated proteins MAP2 and τ. *J. Biol. Chem.* **256**, 8795-8800.

**Saxton, W. M., Stemple, D. L., Leslie, R. J., Salmon, E. D., Zavortink, M. and McIntosh, J. R.** (1984). Tubulin dynamics in cultured mammalian cells. *J. Cell Biol.* **99**, 2175-2186.

**Scherson, T. Z., Kreis, T. E., Schlessinger, J., Littauer, U. Z., Borisy, G. G. and Geiger, B.** (1984). Dynamic interactions of fluorescently labeled microtubule-associated proteins in living cells. *J. Cell Biol.* **99**, 425-434.

**Schulze, E. and Kirschner, M.** (1988). New features of microtubule behaviour observed in vivo. *Nature* **334**, 356-359.

**Schulze, E. and Kirschner, M.** (1986). Microtubule dynamics in interphase cells. *J. Cell Biol.* **102**, 1020-1031.

**Seitz-Tutter, D., Langford, G. M. and Weiss, D. G.** (1988). Dynamic instability of native microtubules from squid axons is rare and independent of gliding and vesicle transport. *Exp. Cell Res.* **33**, 504-512.

**Simon, J. R. and Salmon, E. D.** (1990). The structure of microtubule ends during the elongation and shortening phases of dynamic instability examined by negative-stain electron microscopy. *J. Cell Sci.* **96**, 571-582.

**Simon, J. R. and Salmon, E. D.** (1992). Buffer conditions and non-tubulin factors critically affect the microtubule dynamic instability of sea urchin egg tubulin. *Cell Motil. Cytoskel.* **21**, 1-14.

**Sloboda, R. D., Dentler, W. L. and Rosenbaum, J. L.** (1976). Microtubule-associated proteins and the stimulation of tubulin assembly in vitro. *Biochemistry* **15**, 4497-4505.

**Sloboda, R. D. and Rosenbaum, J. L.** (1979). Decoration and stabilization of intact, smooth-walled microtubules with microtubule-associated proteins. *Biochemistry* **18**, 48-55.

**Soltys, B. J. and Borisy, G. G.** (1985). Polymerization of tubulin in vivo: direct evidence for assembly onto microtubule ends and from centrosomes. *J. Cell Biol.* **100**, 1682-1689.

**Stewart, R. J., Farrell, K. W. and Wilson, L.** (1990). Role of GTP hydrolysis in microtubule polymerization: evidence for a coupled hydrolysis mechanism. *Biochemistry* **29**, 6489-6498.

**Tanaka, E. and Kirschner, M.** (1991). Microtubule behavior in the growth cones of living neurons during axon elongation. *J. Cell Biol.* **115**, 345-363.

**Vallee, R. B. and Bloom, G. S.** (1984). High molecular weight microtubule-associated proteins. *Mod. Cell Biol.* **3**, 21-76.

**Vallee, R. B. and Davis, S. E.** (1983). Low molecular weight microtubule-associated proteins are light chains of microtubule-associated protein 1 (MAP1). *Proc. Nat. Acad. Sci. U.S.A.* **80**, 1342-1346.

**Vallee, R. B. and Shpetner, H. S.** (1990). Motor proteins of cytoplasmic microtubules. *Annu Rev. Biochem.* **59**, 909-932.

**Voter, W. A. and Erickson, H. P.** (1982). Electron microscopy of MAP2 (microtubule-associated protein 2). *J. Ultrastruct. Res.* **80**, 374-382.

**Wadsworth, P. and Salmon, E. D.** (1986). Analysis of the treadmilling model during metaphase of mitosis using fluorescence redistribution after photobleaching. *J. Cell Biol.* **102**, 1032-1038.

**Walker, R. A., Inoue, S. and Salmon, E. D.** (1989). Asymmmetric

behavior of severed microtubules following ultraviolet-microbeam irradiation of individual microtubules in vitro. *J. Cell Biol.* **108**, 931-937.

**Walker, R. A., O'Brien, E. T., Pryer, N. K., Soboeiro, M. F., Voter, W. A., Erickson, H. P. and Salmon, E. D.** (1988). Dynamic instability of individual, MAP-free microtubules analyzed by video light microscopy: rate constants and transition frequencies. *J. Cell Biol.* **107**, 1437-1448.

**Walker, R. A., Pryer, N. K. and Salmon, E. D.** (1991). Dilution of individual microtubules observed in real time in vitro: evidence that cap size is small and independent of elongation rate. *J. Cell Biol.* **114**, 73-81.

*(Received 27 July 1992 - Accepted 3 September 1992)*